

Feature-Scale Modeling of Low-Bias SF₆ Plasma Etching of Si

Luiz Felipe Aguinsky*, Georg Wachter†, Frâncio Rodrigues*, Alexander Scharinger*, Alexander Toifl*, Michael Trupke†, Ulrich Schmid‡, Andreas Hössinger§, and Josef Weinbub*

*Christian Doppler Laboratory for High Performance TCAD,

Institute for Microelectronics, TU Wien, Gußhausstraße 27-29, 1040 Wien, Austria

†Faculty of Physics, University of Vienna, VCQ, Boltzmanngasse 5, 1090, Wien, Austria

‡Institute of Sensor and Actuator Systems, TU Wien, Gußhausstraße 27-29, 1040 Wien, Austria

§Silvaco Europe Ltd., Compass Point, St Ives, Cambridge, PE27 5JL, United Kingdom

Email: aguinsky@iue.tuwien.ac.at

Abstract—Low-bias etching of Si using SF₆ plasma is a valuable tool in the manufacturing of semiconductor and MEMS devices. This kind of etching has strong isotropic tendencies, since the low voltage bias does not provide enough vertical acceleration and kinetic energy to the ions. This near-isotropy can be difficult to precisely reproduce in a topography simulation, since experimentally realized surfaces cannot be reproduced by a strictly isotropic velocity model. We present a three-dimensional top-down Monte Carlo particle tracing model for calculating the velocity field in a level-set based simulation. We compare it to profilometer measurements of optical cavities, which are of interest to quantum science, fabricated using a two-step SF₆ plasma etching process. We contrast our approach to conventional models: a strictly isotropic model and a bottom-up direct flux calculation. We show that our top-down model leads to a more accurate description of the final surface by introducing a sticking probability at the surface and also multiple reflections. We are able to reproduce cavities fabricated from different initial photoresist configurations with a single silicon etch rate ($V_{Si} = 2.15 \mu\text{m min}^{-1}$), while the conventional models require a separate V_{Si} for each photoresist geometry. The model successfully reproduces a Si/photoresist selectivity of 10, which, combined with the low calibrated sticking probability ($\beta_{Si} = 7.5\%$), corroborates with F radicals being the main drivers of etching. By exploring the state of the surface after the first etch step, which is not readily available experimentally, we anticipate the phenomena of underetching and photoresist tapering.

Index Terms—Plasma etching, process TCAD, topography simulations, ray-tracing, level-set method, SF₆ plasma

I. INTRODUCTION

Plasma etching of silicon (Si) using sulphur hexafluoride (SF₆) gases is a standard technology in modern semiconductor fabrication processes [1], such as memory devices, microelectromechanical systems (MEMS), and as a sub-step in the Bosch process [2], [3]. Under low-bias conditions, SF₆ plasma etching is known to have a near-isotropic behavior yielding profiles similar, but not identical, to those obtained by wet etching [4]. This is due to the low voltage bias between the plasma and the wafer not accelerating the ions to a large degree. Therefore, the anisotropic component, caused by the kinetic energy of the vertical ions, is minimal [5]. The near-isotropic behavior has proven to be useful in, e.g.,

optical applications, where surface cleanliness requirements favor plasma etching over wet etching [6].

Feature-scale topography simulations are part of process technology computer-aided design (TCAD) workflows which enable, among others, the investigation of etched or deposited materials [7]. While two-dimensional feature-scale modeling of SF₆ etching of Si has been reported for anisotropic, high-bias conditions [8], low-bias etching provides a different set of challenges for accurately modeling the topography since the final surfaces are not ideal, that is, they are not equivalent to surfaces etched by a perfectly isotropic process.

Here, we present a three-dimensional feature-scale model tailored to the challenge of the low-bias, near-isotropic regime of SF₆ etching of Si. This is achieved using *top-down* Monte Carlo particle tracing [9] including multiple reflections. Our model is contrasted to conventional, strictly isotropic, and bottom-up models [10]. Our top-down model and the conventional models are summarized visually in Fig. 1. The simulated profile is calibrated to an experimentally measured cavity, fabricated with a two-step SF₆ low-bias plasma etching process, which is of relevance for the development of optical resonators for quantum science [6]. We then interpret our model with respect to chemical etching mechanisms. Finally, using calibrated simulations, we are able to investigate the state of the surface after the first etch step, a state which is not readily available experimentally, thereby also underlining one of the key advantages of process TCAD simulations.

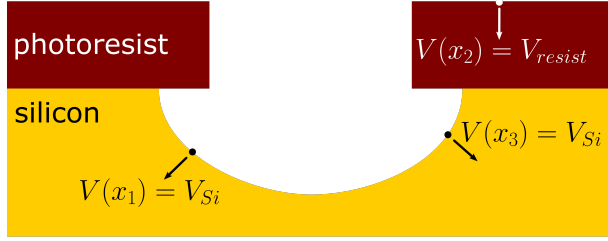
II. METHOD

In order to simulate the time evolution of an etched surface, we employ the level-set method [11]. The evolving surface is represented as the zero level-set of the signed distance function ϕ . Its propagation is described by the solution of the following level-set equation for ϕ :

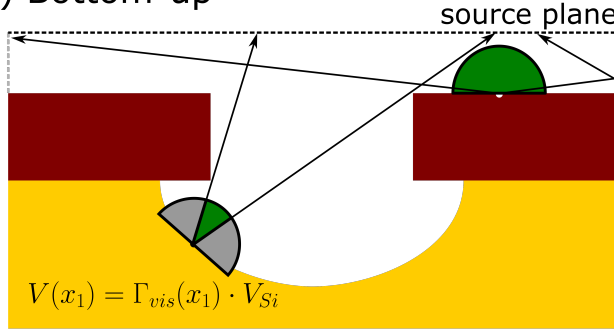
$$\frac{\partial\phi(x,t)}{\partial t} + V(x)|\nabla\phi(x,t)| = 0. \quad (1)$$

The solution of (1) is performed by Silvaco's three-dimensional process TCAD tool *Victory Process* [12]. The modeling of surface reactions and subsequent local etch rates is achieved via the velocity field $V(x)$, as discussed below.

a) Strictly isotropic



b) Bottom-up



c) Top-down

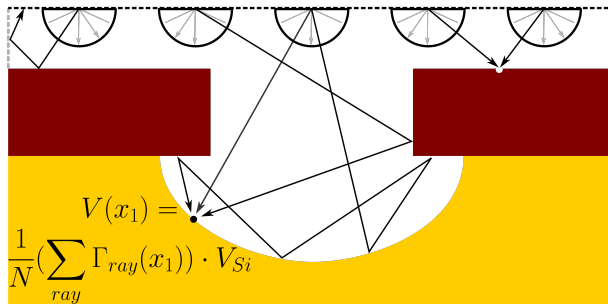


Fig. 1: Illustration of models for the local surface propagation rate $V(x)$. Our top-down model (c) is contrasted to the conventional strictly isotropic (a) and bottom-up (b) procedures.

As reported previously [1], under low-bias conditions the etching is expected to be near-isotropic. Such etching is mostly performed by highly reactive isotropic F radicals generated in the plasma. They can etch both Si and the photoresist. Due to the low-bias, the directional component caused by the vertically accelerated ions is minimal.

The precise nature of the low-bias behavior requires accurate modelling. In Fig. 1, we present an illustration of three possible approaches to generate $V(x)$ for an isotropic etchant. The straightforward approach, i.e., strictly isotropic, is represented in Fig. 1.a). In this case, the same constant velocity is applied to all exposed surface elements of the same material. This results in a surface equivalent to that processed by ideal isotropic wet etching [13]. Therefore, in the strictly isotropic case the velocity $V_{S-I}(x)$ is simply a function of the involved material (either Si or the resist):

$$V_{S-I}(x) = V_{Si/resist}. \quad (2)$$

However, since plasma etching is a gas-phase method, the etchant distribution is not always identical across the surface. A more complex model thus requires the construction of an approximation to the local flux of etchant particles $\Gamma(x)$ in order to more accurately model $V(x)$. An elementary way of calculating $\Gamma(x)$, represented in Fig. 1.b), assumes that the incoming particle stream originates isotropically from a source plane. Subsequently, the local visibility of this plane is calculated in a bottom-up fashion for the hemisphere above each surface element [10], leading to a local flux $\Gamma_{vis}(x)$ which is normalized to 1 for a fully-exposed element. The final velocity is the plane-wafer etch rate weighted with $\Gamma_{vis}(x)$. This model allows the capture of some topography-dependent effects, however, it does not take reflections into account. The velocity field in the bottom-up model $V_{B-U}(x)$ is:

$$V_{B-U}(x) = \Gamma_{vis}(x) \cdot V_{Si/resist}. \quad (3)$$

We propose a physically richer top-down model, as shown in Fig. 1.c), supporting multiple reflections according to the sticking probability β . This is achieved by a Monte Carlo sampling of N particles of a single type, which are generated isotropically in the source plane and carry a flux payload Γ_{ray} . Their trajectories through the domain are computed using a ray-tracing method and reflective boundary conditions. When a simulated particle hits the surface, it is terminated, leaving its payload Γ_{ray} at the surface site. A new reflected particle is generated, following an isotropic reflection distribution and having a new payload Γ_{ref} mediated by $\beta_{Si/resist}$, i.e.:

$$\Gamma_{ref} = (1 - \beta_{Si/resist}) \cdot \Gamma_{ray}. \quad (4)$$

Finally, the local velocity of the surface is calculated from the normalized sum of $\Gamma_{ray}(x)$ for all particles, both generated in the source plane and reflected, and from the plane-wafer etch rate V . This effectively generalizes the two previous models, as the strictly isotropic approach is recovered with the limit $\beta \rightarrow 0^+$, and the bottom up, with $\beta \rightarrow 1^-$. In summary, the velocity for the top-down model V_{T-D} is:

$$V_{T-D}(x) = \frac{1}{N} \left(\sum_{ray} \Gamma_{ray}(x) \right) \cdot V_{Si/resist}. \quad (5)$$

The isotropic source and reflection distributions are motivated by the low-bias characteristics of the etching process. That is, the etchants are not accelerated and interact with the surface in a diffuse manner. This is consistent with the expected mechanism of etching: The generation of F radicals in the plasma which chemically etch the surface [14].

Therefore, the free parameters are the silicon plane-wafer etch rates V_{Si} for the first and second steps, and the photoresist etch rate V_{resist} . In addition, the top-down model has as parameters the sticking coefficients β_{Si} and β_{resist} . Although this indicates that the top-down model is successful due to its additional fitting parameters, we will discuss in the next section that the conventional models require different values of V_{Si} for each individual initial photoresist geometry, which is not straightforwardly justifiable from a physical standpoint.

Thus, the top-down model involves not only an equivalent number of parameters, but also its values can be physically interpreted and compared to reported results [15].

III. RESULTS

To validate the proposed model, we compare it to three-dimensional profilometer measurements of experimentally fabricated structures [6]. Multiple cavities were etched simultaneously on Si using a two-step SF₆ plasma etching process, each cavity under a different initial photoresist cylindrical opening d . We studied three different cavities with a respective d of 12.4 μm , 34 μm , and 52 μm . The first etch step was performed for 320 seconds and took place having the photoresist present. After photoresist removal using acetone, a second etch step was applied for 48 minutes. We manually calibrate the simulations to the final topography of the fabricated surfaces, i.e., after photoresist removal and the second etch step.

The calibrated parameters for the top-down model are presented in Tab. I. For the strictly isotropic and bottom-up models, the same V_{resist} and second etch step V_{Si} are applied, however, each cavity requires an individually calibrated first step V_{Si} , presented in Tab. II. A cross-section contrasting the simulation approaches to the experiment is shown Fig. 2.

TABLE I: Calibrated parameters for top-down simulation.

Parameter	Calibrated value
First etch step V_{Si}	$2.15 \mu\text{m min}^{-1}$
Second etch step V_{Si}	$0.66 \mu\text{m min}^{-1}$
V_{resist}	$0.21 \mu\text{m min}^{-1}$
β_{Si}	7.5 %
β_{resist}	6.1 %

TABLE II: Calibrated first etch step V_{Si} for each photoresist opening d for the strictly isotropic and bottom-up simulations.

Opening d	Strictly isotropic first V_{Si}	Bottom-up first V_{Si}
12.4 μm	$1.45 \mu\text{m min}^{-1}$	$23.0 \mu\text{m min}^{-1}$
34 μm	$1.94 \mu\text{m min}^{-1}$	$6.0 \mu\text{m min}^{-1}$
52 μm	$2.09 \mu\text{m min}^{-1}$	$3.6 \mu\text{m min}^{-1}$

The results show the failure of the bottom-up model, since it cannot correctly capture the curvature, i.e., it underestimates the etch rates at the sidewalls. The strictly isotropic model has a very similar shape to the experiment and to the top-down model, in particular for the cavity with $d = 12.4 \mu\text{m}$. However, since it applies the same rate to all exposed regions, the bottom of the cavity, i.e., the area under the original photoresist opening, remains unrealistically flat. Since the strictly isotropic model is equivalent to having $\beta = 0$, the similarity of the strictly isotropic model to the experimental profile is evidence that a low β is expected, as confirmed in the calibrated values on Tab. I. However, the perfectly flat profiles at the bottom are not observed in the experiment [6] and, additionally, cause the surface to be unsuited for optical applications and incompatible with further numerical investigation [16].

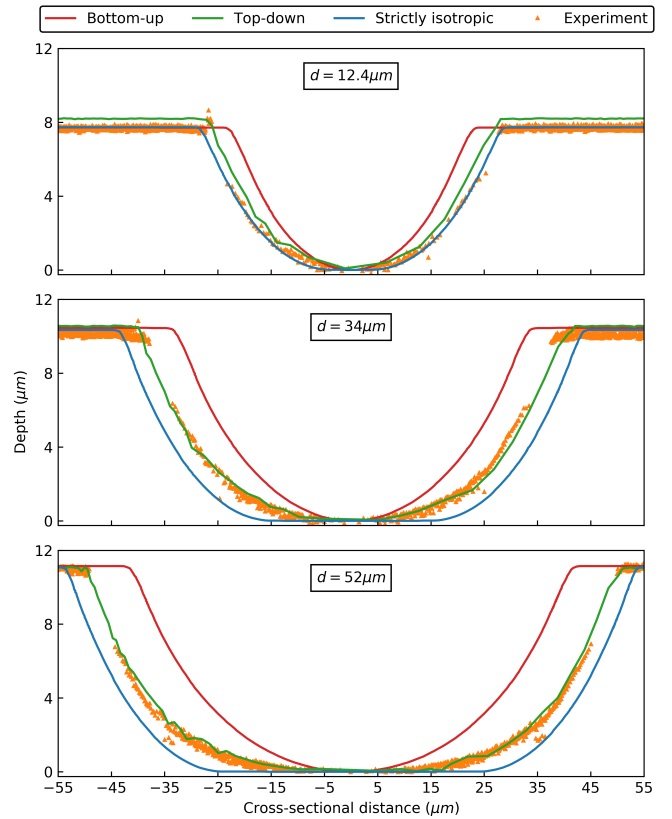


Fig. 2: Cross-sections of the simulated surfaces using the models from Fig. 1 and measurements of experimentally fabricated surfaces with different initial photoresist openings d using a two-step low-bias SF₆ plasma etching process.

In addition to the observed correspondence with the experiment shown in Fig. 2, the top-down model offers a significant advantage. Only a single V_{Si} for the first etch step is required, whereas separate values are required for each cavity for the conventional models. This indicates that the top-down model more accurately captures the real chemical processes involved in low-bias SF₆ etching. The SF₆ plasma is known to be a source of highly reactive F radicals which chemically etch the surface [14]. This is supported by our results, since we can reproduce the topography with a single Monte Carlo particle (representing the F radicals) with a low, but not zero, β which is consistent with reported values [15].

The calibrated parameters in Tab. I show a lower V_{Si} for the second etch step. This is expected due to the effect of reactor loading [1], [17]. In the second etch step there is no photoresist, therefore, there is a larger wafer surface available to consume the reactants. This reduces their local supply, decreasing V_{Si} . The change in reactor loading during the first etch step is neglected, since the increase in exposed Si is small compared to the total wafer area covered by the photoresist. Additionally, the values show a Si/photoresist selectivity of 10, which is consistent with reported results [18].

Using topography simulation, we are able to explore states which are not readily available experimentally. In particular, the profile after the first etch step but before photoresist removal, shown in Fig. 3. For the top-down approach, this figure is obtained with the parameters from Tab. I. The parameters were re-calibrated for the bottom-up and strictly isotropic models in order to achieve the same depth.

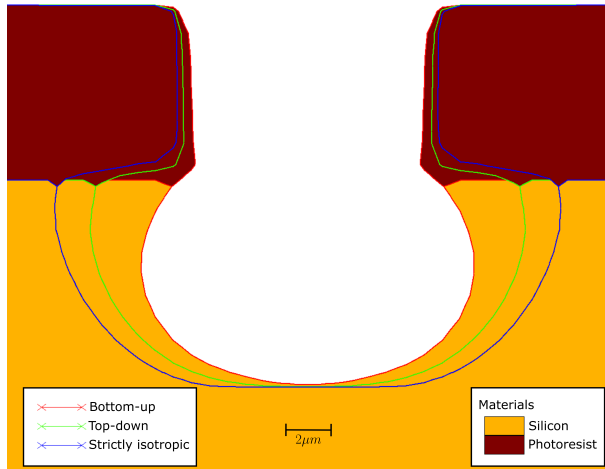


Fig. 3: Simulated etched surfaces for a cavity with photoresist $d = 12.4 \mu\text{m}$ showing underetching and photoresist tapering.

We can see that the conventional bottom-up approach has fundamental limitations. The shape is more bulbous, which leads to the incorrect final curvature seen in Fig. 2. Additionally, the bottom-up model is unable to capture underetching, i.e., the etching of Si directly below the photoresist, which is experimentally a known feature of low-bias SF_6 etching [1]. For the strictly isotropic approach, the flatness of the bottom is even clearer at this step. As discussed previously, this makes the strictly isotropic approach unsuitable. Finally, we would like to highlight that our simulations indicate the presence of photoresist tapering during the etching, which is a phenomenon of interest for further process improvement.

IV. SUMMARY

We have presented a physically rich, calibrated, top-down model to calculating the velocity field $V(x)$ for the surface evolution of low-bias SF_6 plasma etching of Si. We show that the conventional strictly isotropic and bottom-up approaches are insufficient to represent the experimental topography. By introducing multiple reflections and a sticking probability β , the top-down model is able to more accurately represent the final surfaces while simultaneously using the same parameter set for multiple geometries. The success of the top-down approach provides insight into the surface chemistry of SF_6 plasma etching, highlighting the importance of F radicals as the drivers of chemical etching. The calibrated parameter set captures the effect of reactor loading and reports values of β and Si/photoresist selectivity consistent with the literature. Using our calibrated simulations, we are able to explore a state which is not readily accessible experimentally, i.e., after

the first etch step and before photoresist removal, featuring the expected phenomena of underetching and photoresist tapering.

ACKNOWLEDGMENT

The financial support by the Austrian Federal Ministry for Digital and Economic Affairs, the National Foundation for Research, Technology and Development, and the Christian Doppler Research Association is gratefully acknowledged. M. Trupke and G. Wachter gratefully acknowledge support from the EU H2020 framework programme (QuanTELCO, 862721), the FWF (SiC-EiC, I 3167-N27), and the FFG (QSense4Power, 877615).

REFERENCES

- [1] V. M. Donnelly and A. Kornblit, "Plasma Etching: Yesterday, Today, and Tomorrow," *Journal of Vacuum Science & Technology A: Vacuum, Surfaces, and Films*, vol. 31, no. 5, p. 050825, 2013.
- [2] C. Waits *et al.*, "Microfabrication of 3D Silicon MEMS Structures using Gray-Scale Lithography and Deep Reactive Ion Etching," *Sensors and Actuators A: Physical*, vol. 119, no. 1, pp. 245–253, 2005.
- [3] F. Patocka, C. Schneidhofer, N. Dörr, M. Schneider, and U. Schmid, "Novel Resonant MEMS Sensor for the Detection of Particles with Dielectric Properties in Aged Lubricating Oils," *Sensors and Actuators A: Physical*, vol. 315, p. 112290, 2020.
- [4] P. Panduranga, A. Abdou, Z. Ren, R. H. Pedersen, and M. P. Nezhad, "Isotropic Silicon Etch Characteristics in a Purely Inductively Coupled SF_6 Plasma," *Journal of Vacuum Science & Technology B, Nanotechnology and Microelectronics: Materials, Processing, Measurement, and Phenomena*, vol. 37, no. 6, p. 061206, 2019.
- [5] M. A. Lieberman and A. J. Lichtenberg, *Principles of Plasma Discharges and Materials Processing*. John Wiley & Sons, 2005.
- [6] G. Wachter *et al.*, "Silicon Microcavity Arrays with Open Access and a Finesse of Half a Million," *Light: Science & Applications*, vol. 8, no. 1, pp. 1–7, 2019.
- [7] X. Klemenshchits, S. Selberherr, and L. Filipovic, "Modeling of Gate Stack Patterning for Advanced Technology Nodes: A Review," *Micro-machines*, vol. 9, no. 12, p. 631, 2018.
- [8] R. J. Belen, S. Gomez, M. Kiehlbauch, D. Cooperberg, and E. S. Aydil, "Feature-Scale Model of Si Etching in SF_6 Plasma and Comparison with Experiments," *Journal of Vacuum Science & Technology A: Vacuum, Surfaces, and Films*, vol. 23, no. 1, pp. 99–113, 2005.
- [9] A. Scharinger, P. Manstetten, A. Hössinger, and J. Weinbub, "Generative Model Based Adaptive Importance Sampling for Flux Calculations in Process TCAD," in *Proceedings of the International Conference on Simulation of Semiconductor Processes and Devices (SISPAD)*, 2020, pp. 39–42.
- [10] P. Manstetten, J. Weinbub, A. Hössinger, and S. Selberherr, "Using Temporary Explicit Meshes for Direct Flux Calculation on Implicit Surfaces," *Procedia Computer Science*, vol. 108, pp. 245–254, 2017.
- [11] J. A. Sethian, *Level Set Methods and Fast Marching Methods: Evolving Interfaces in Computational Geometry, Fluid Mechanics, Computer Vision, and Materials Science*. Cambridge University Press, 1999.
- [12] Silvaco, "Victory Process," 2021. [Online]. Available: www.silvaco.com/tcad/victory-process-3d/
- [13] J. Miao, *Silicon Micromachining*. Boston, MA: Springer US, 2008, pp. 1840–1846.
- [14] D. L. Flamm, V. M. Donnelly, and J. A. Mucha, "The Reaction of Fluorine Atoms with Silicon," *Journal of Applied Physics*, vol. 52, no. 5, pp. 3633–3639, 1981.
- [15] V. M. Donnelly, "Reactions of Fluorine Atoms with Silicon, Revisited, Again," *Journal of Vacuum Science & Technology A: Vacuum, Surfaces, and Films*, vol. 35, no. 5, p. 05C202, 2017.
- [16] D. Kleckner, W. T. Irvine, S. S. Oemrawsingh, and D. Bouwmeester, "Diffraction-Limited High-Finesse Optical Cavities," *Physical Review A*, vol. 81, no. 4, p. 043814, 2010.
- [17] C. Mogab, "The Loading Effect in Plasma Etching," *Journal of the Electrochemical Society*, vol. 124, no. 8, p. 1262, 1977.
- [18] K. R. Williams, K. Gupta, and M. Wasilik, "Etch Rates for Micromachining Processing-Part II," *Journal of Microelectromechanical Systems*, vol. 12, no. 6, pp. 761–778, 2003.